Supplementary Materials

Regioselective Hydroxylation of Rhododendrol by CYP102A1 and Tyrosinase

Chan Mi Park [1], Hyun Seo Park [1], Gun Su Cha [2], Ki Deok Park [3], and Chul-Ho Yun [1,*]

[1] School of Biological Sciences and Technology, Chonnam National University, 77 Yongbongro, Gwangju 61186, Republic of Korea; cmpark0710@gmail.com (C.M.P); hs6471@naver.com (H.S.P)
[2] Namhae Garlic Research Institute, 2465-8 Namhaedaero, Namhae, Gyeongsangnamdo, 52430, Republic of Korea; gscha450@gmail.com
[3] Gwangju Center, Korea Basic Science Center, 77 Yongbongro, Gwangju 61186, Republic of Korea; kdpark@kbsi.re.kr
* Correspondence: chyun@chonnam.ac.kr

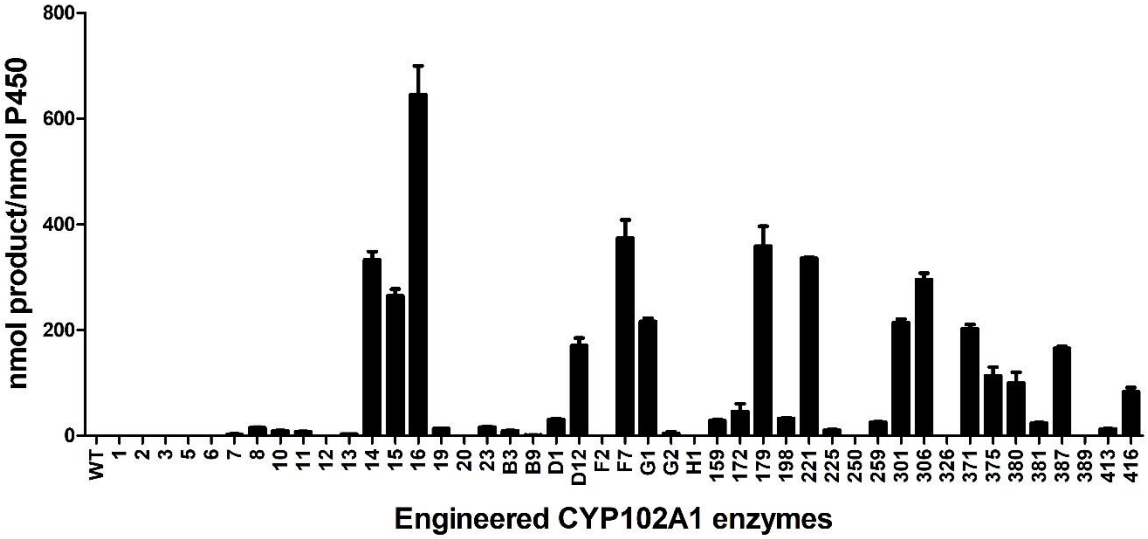

Figure S1. Total turnover numbers of engineered CYP102A1 enzymes. The catalytic activity of CYP102A1 WT and 45 engineered enzymes were measured by HPLC. The reaction mixtures contained 0.2 μM enzymes, 200 μM RD, and NGS in 250 μL of 100 potassium phosphate buffer (pH 7.4) and were incubated at 37 °C for 30 min. The values are represented as the mean with SEM of triple measurements.

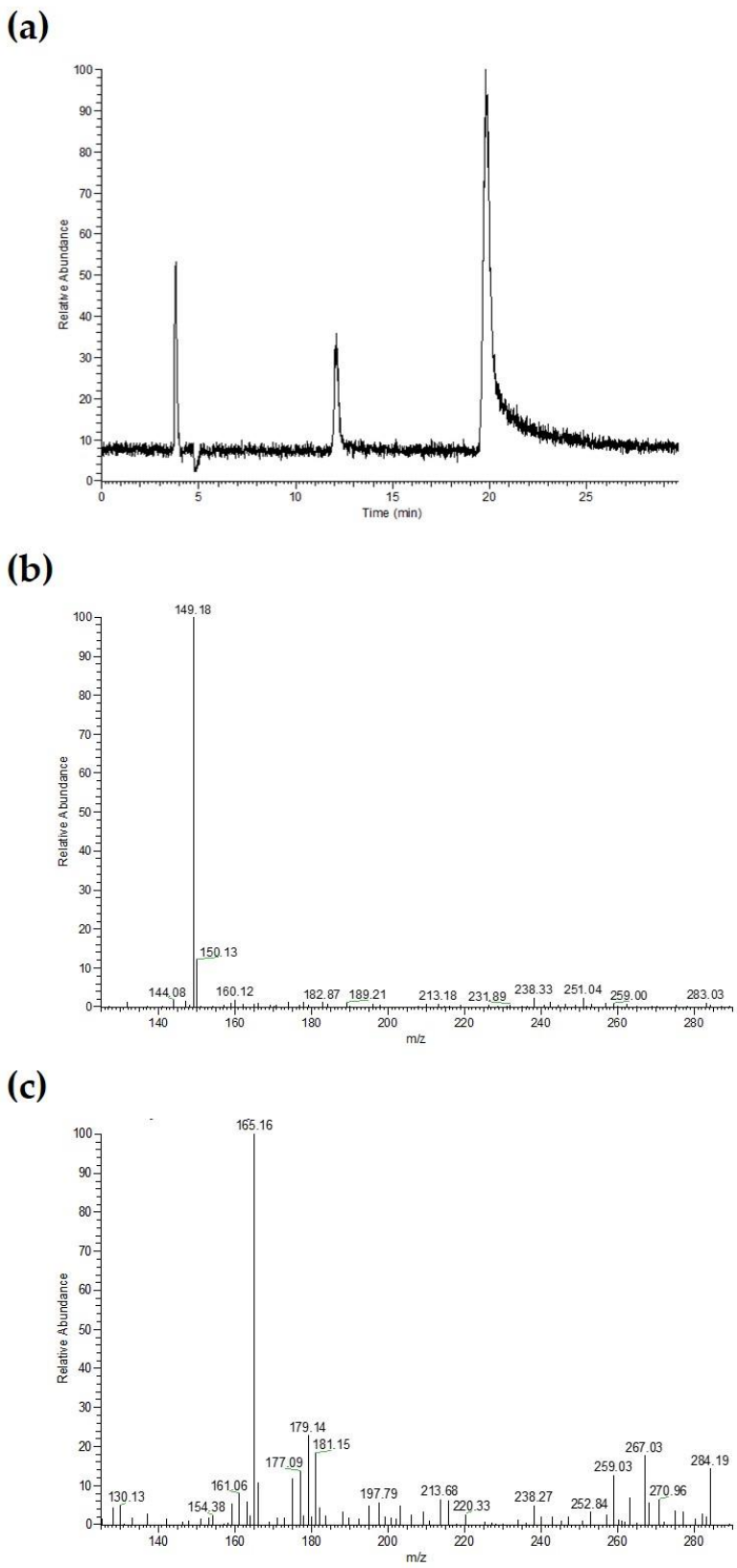

Figure S2. Total ion chromatography and mass scan of RD and product of M16. (a) Retention times of RD and product were 20 and 12 min respectively. (b) The m/z value for $[M]^+$ of RD was 149. (c) The m/z value for $[M]^+$ of product was 165.

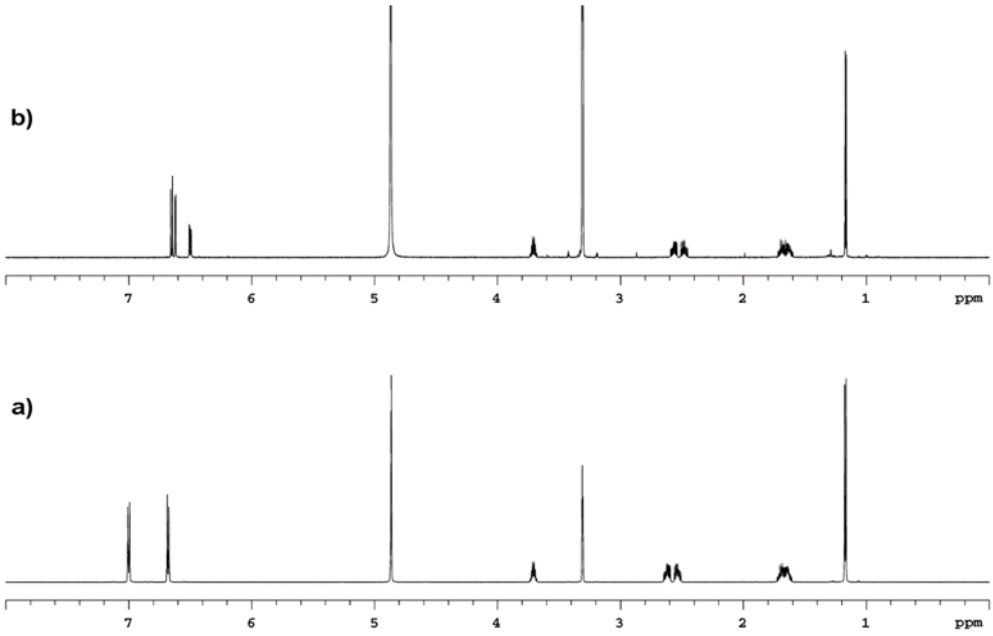

Figure S3. ^{1}H NMR spectra of RD (a) and the major product of M16 (b).

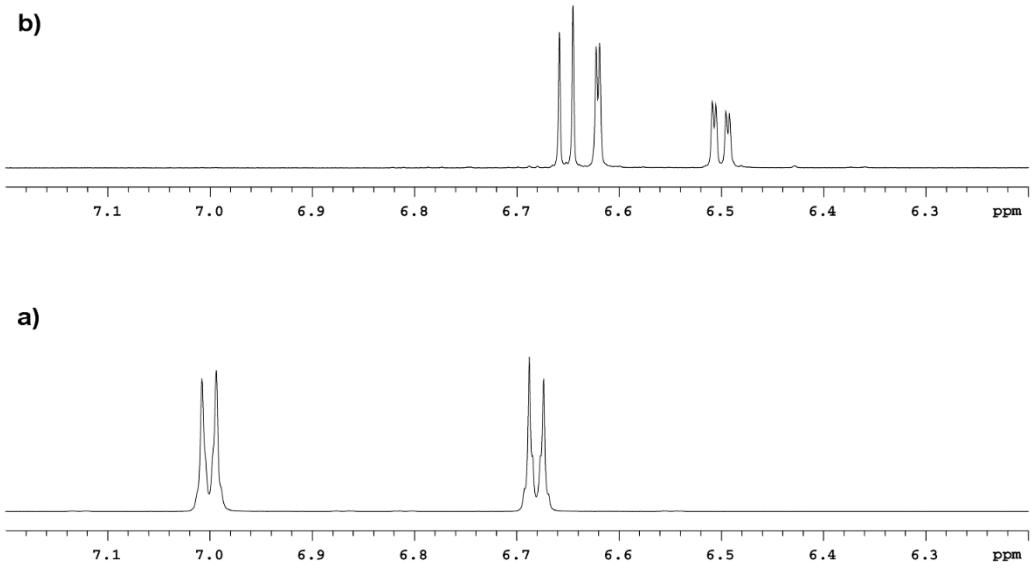

Figure S4. Comparison of aromatic region in the ^{1}H NMR spectra of RD (a) and the major product of M16 (b).

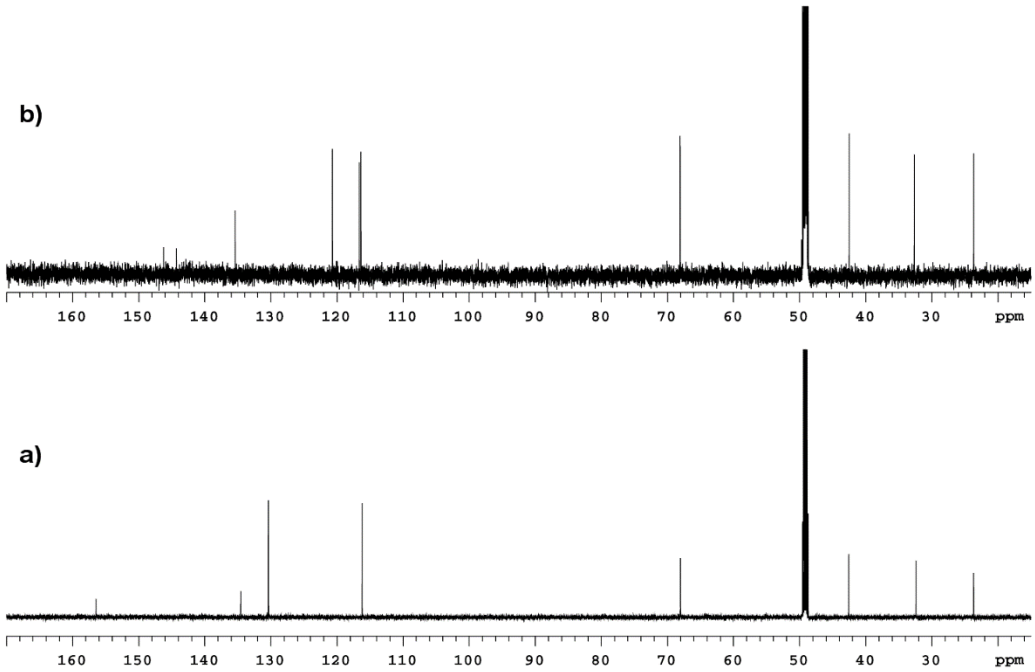

Figure S5. ^{13}C NMR spectra of RD (a) and the major product of M16 (b).

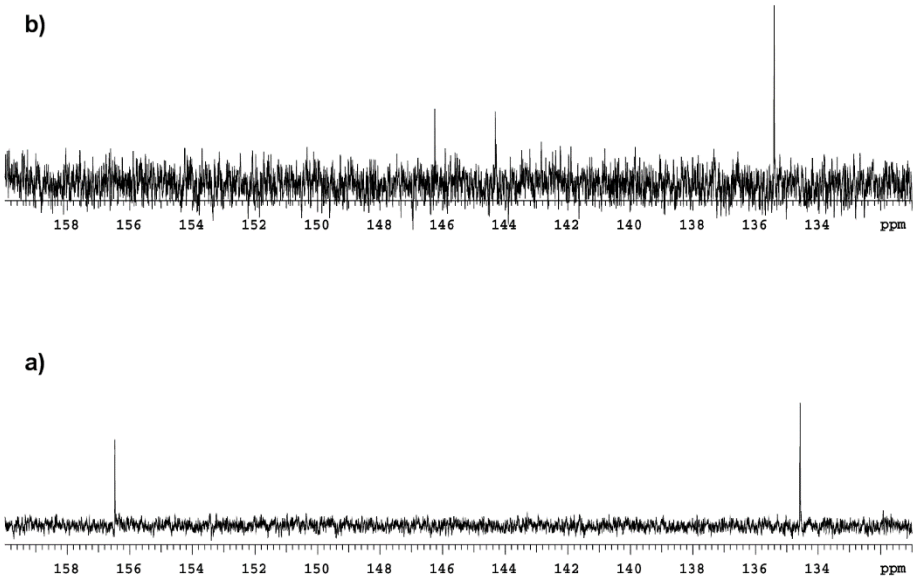

Figure S6. Comparison of quaternary peaks in the ^{13}C NMR spectra of RD (a) and the major product of M16 (b).

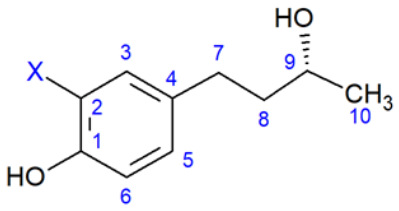

	X
RD (M0)	H
RD-catechol (M1, M2)	OH

Figure S7. Chemical structures of RD and RD-catechol. M0, M1, and M2 indicate RD, product of M16, and product of Ty, respectively.

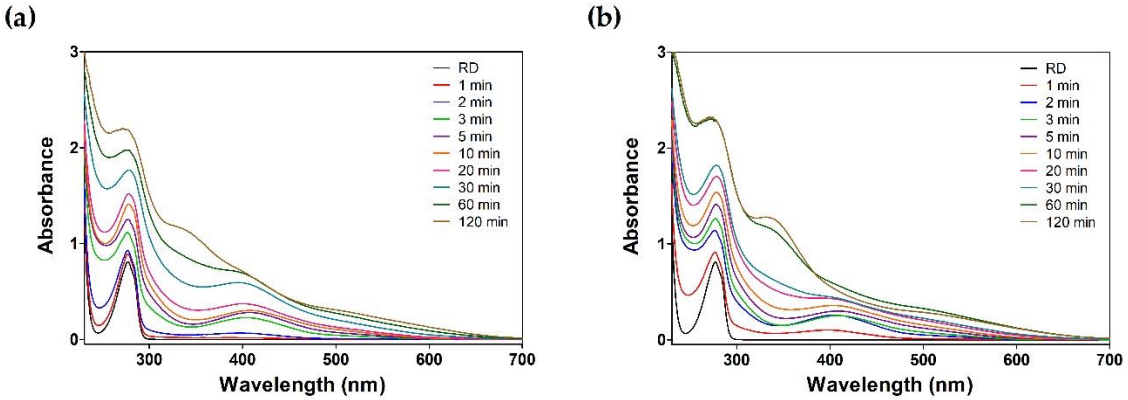

Figure S8. RD-quinone formation by Ty was analyzed by UV-Vis spectrophotometer. Absorbance changes were measured at range of 230-700 nm. The reaction mixtures contained 20 units of Ty and 500 μM RD in 1 mL of 100 mM potassium phosphate buffer (pH 6.5) and were incubated at 25 °C (a) and 37 °C (b) for indicated time.

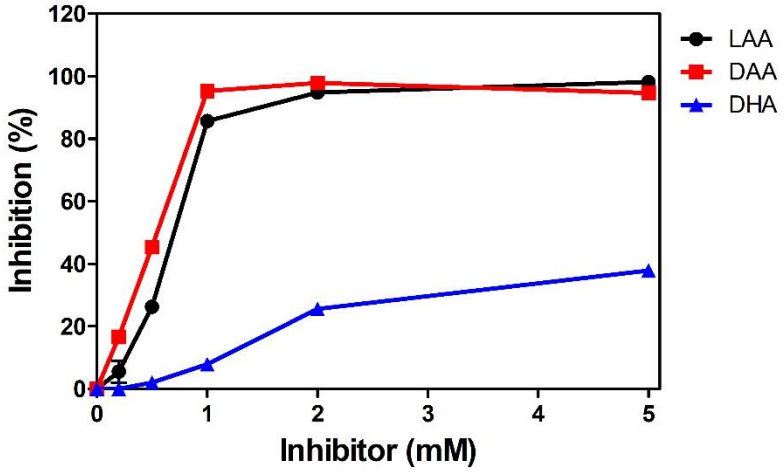

Figure S9. Inhibition of RD-quinone formation by L-ascorbic acid (LAA), D-ascorbic acid (DAA), and dehydroascorbic acid (DHA) at 25 °C. The reaction mixtures contained 20 units of Ty; 500 μM RD; and 1 mM LAA, DAA, or DHA in 1 mL of 100 mM of potassium phosphate buffer (pH 6.5), and were incubated at 25 for 30 min. The inhibitory effects were measured using UV-vis spectrometer at 400 nm.

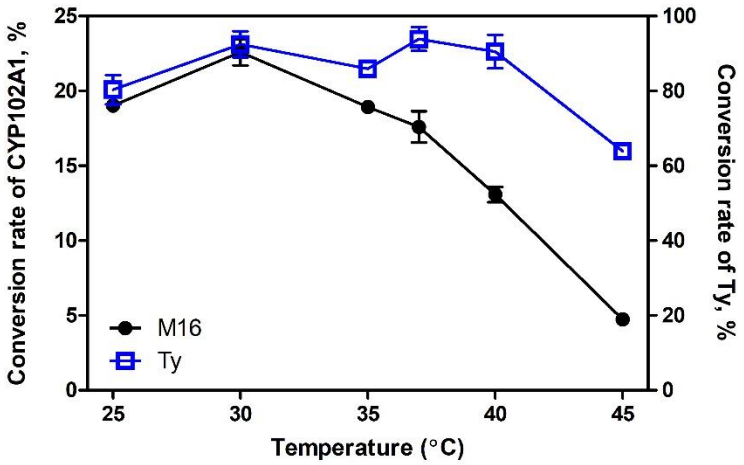

Figure S10. Effects of temperature on conversion rate of CYP102A1 and Ty. The CYP102A1 reaction mixtures contained 0.2 μM M16, 500 μM RD, and NGS in 250 μL of 100 potassium phosphate buffer (pH 7.4). The Ty reaction mixtures contained 5 units of Ty, 500 μM RD, and 10 mM LAA in 250 μL of 100 mM potassium phosphate buffer (pH 6.5). These reaction mixtures were incubated at 25, 30, 35, 37, 40, or 45 °C for 30 min. The products of CYP102A1 and Ty were analyzed by HPLC. The values are represented as the mean with SEM of triple measurements.

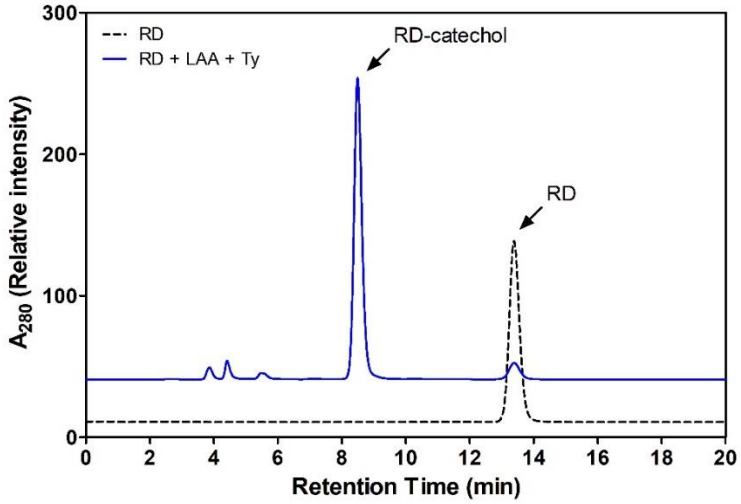

Figure S11. HPLC chromatogram of RD and RD-catechol produced by Ty. The reaction mixture contained five units of Ty, 500 μM RD, and 10 mM LAA. RD and RD-catechol eluted at 13.4 and 8.4 min, respectively.

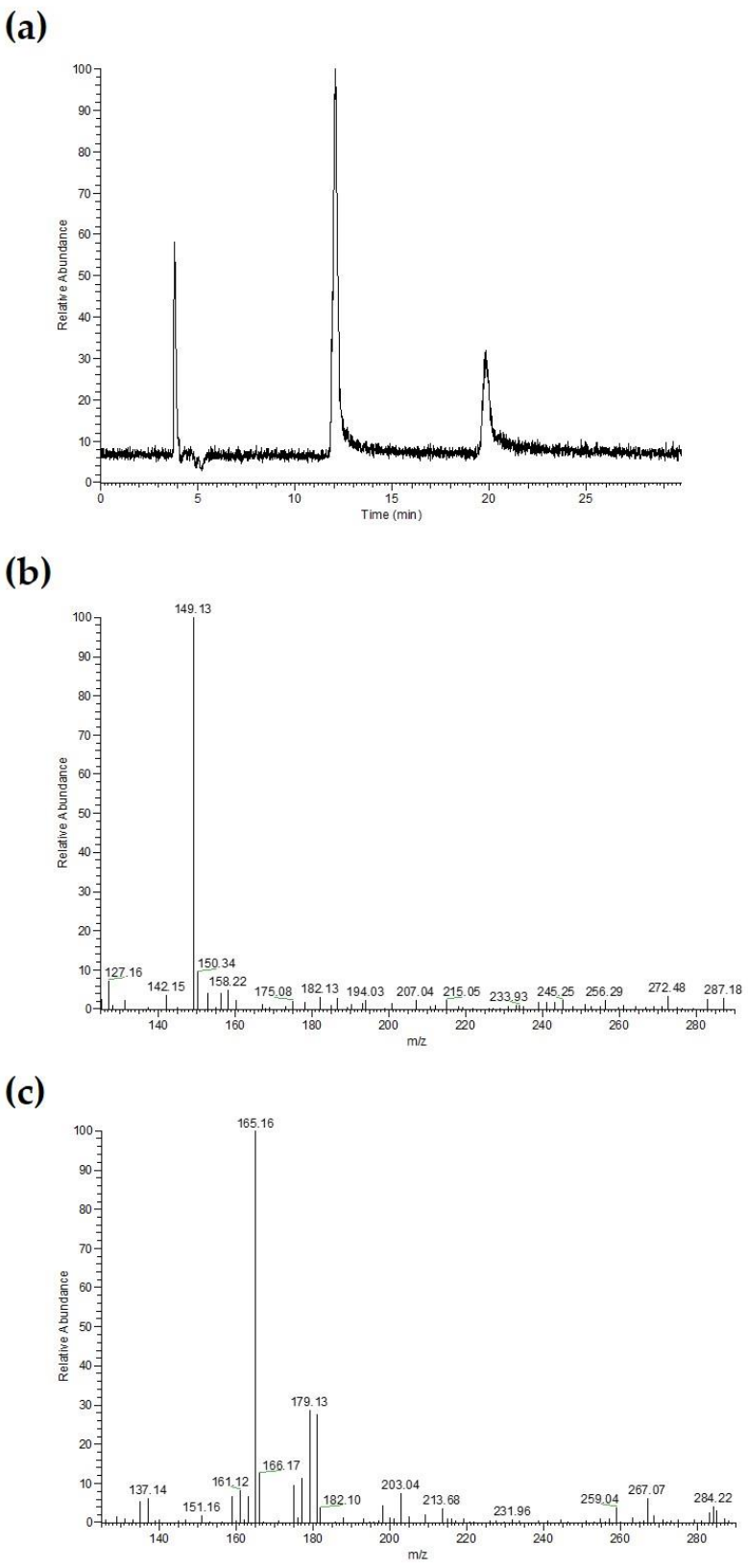

Figure S12. Total ion chromatography and mass scan of RD and product of Ty. (a) Retention times of RD and product were 20 min and 12 min respectively. (b) The m/z value for $[M]^+$ of RD was 149. (c) The m/z value for $[M]^+$ of product was 165.

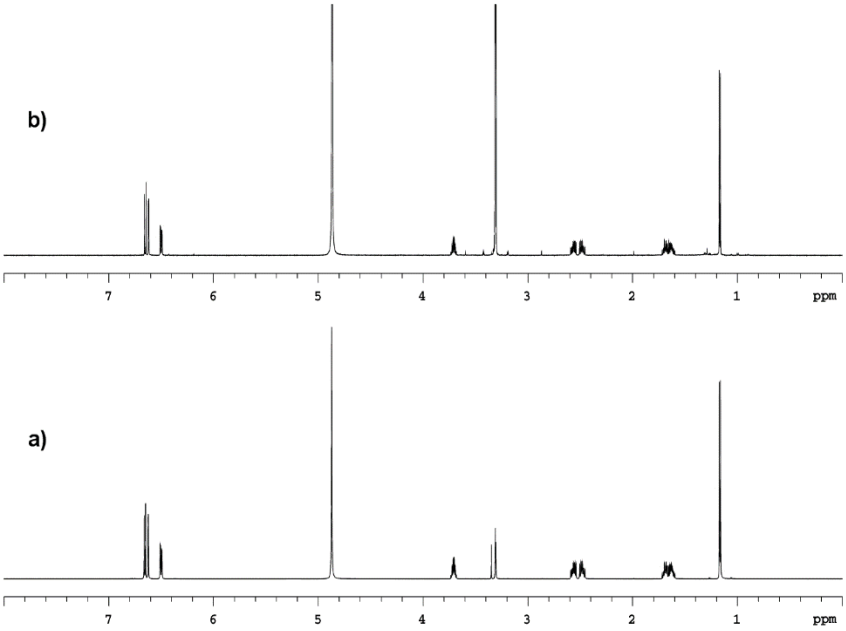

Figure S13. ^{1}H NMR spectra of products of M16 (a) and Ty (b).

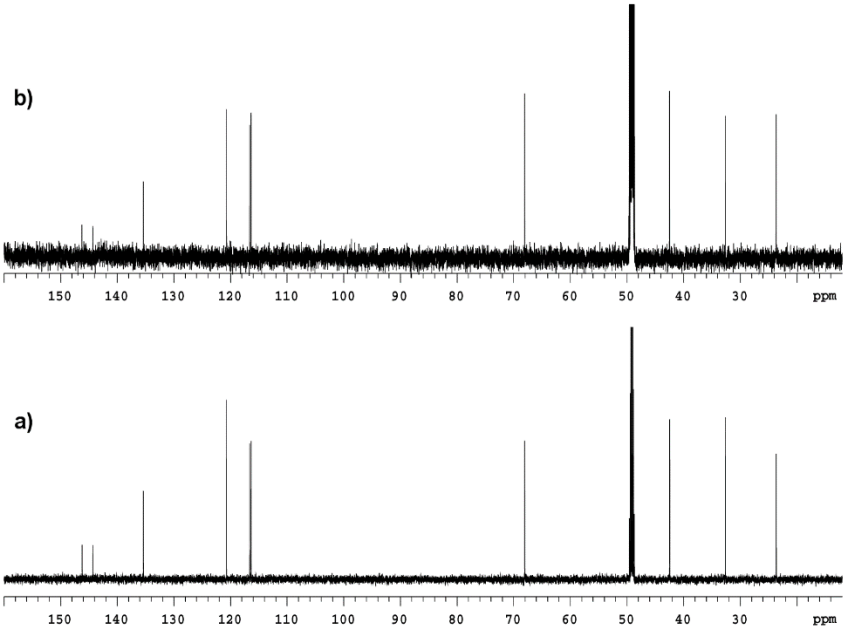

Figure S14. ^{13}C NMR spectra of products of M16 (a) and Ty (b).

Table S1. ^{1}H and ^{13}C chemical shifts of RD and RD-catechol.

Location	RD (M0[a])		RD-catechol (M1, M2[a])	
	^{1}H(d), ppm	^{13}C(d), ppm	^{1}H(d), ppm	^{13}C(d), ppm
1	-	156.482	-	144.318
2	6.681 (d, 2H, J=8.53Hz)	116.217	-	146.256
3	7.001 (d, 2H, J=8.53Hz)	130.392	6.623 (d, 1H, J=2.06Hz)	116.393
4	-	134.579	-	135.407
5	same as 3[b]	same as 3[b]	6.505 (dd, 1H, J=8.03, 2.06Hz)	120.711
6	same as 2[b]	same as 2[b]	6.651 (d, 1H, J=8.03Hz)	116.638
7	2.578(m, 2H)	32.404	2.524(m, 2H)	32.606
8	1.666(m, 2H)	42.584	1.658(m, 2H)	42.495
9	3.709(m, 1H)	68.056	3.709(m, 1H)	68.095
10	1.171 (d, 3H, J=6.14Hz)	23.667	1.168 (d, 3H, J=6.31Hz)	23.666

[a]M0, M1 and M2 indicate RD, product of M16, and product of Ty, respectively.

[b]The locations 2 and 6 (and locations 3 and 5) of RD are chemically and magnetically equivalent with ^{1}H and ^{13}C chemical shifts.

Table S2. Changed amino acid residues of the engineered CYP102A1 enzymes used in this study [a].

Enzyme	Changed amino acid(s)
1	F87A
2	A264G
3	F87A/A264G
5	R47L/Y51F/A264G
6	R47L/Y51F/F87A
7	R47L/Y51F/F87A/A264G
8	A74G/F87V/L188Q
10	R47L/F87V/L188Q
11	R47L/F87V/L188Q/E267V
12	R47L/L86I/L188Q/E267V
13	R47L/L86I/F87V/L188Q
14	R47L/F87V/E143G/L188Q/E267V
15	R47L/E64G/F87V/E143G/L188Q/E267V
16	R47L/F81I/F87V/E143G/L188Q/E267V
19	F162I
20	F162I/M237I
23	F162I/H236R
B3	R47L/F81I/F87V/E143G/I153T/K187Q/ L188Q/N192I/K202Q/E267V
B9	R47L/F81I/F87V/E143G/L188Q/K224R/E267V/G271D/V281A/Q403K
D1	R47L/F81I/F87V/Y115C/E143G/I174S/L188Q/E267V/T268A/Y313F
D12	R47L/S72C/F81I/F87V/E143G/ K187S/L188Q/E267V
F2	R47L/Q73R/F81I/F87V/S108N/E143G/L188Q/I220M/E267V
F7	F173C/N186K/K187Q
G1	R47L/F81I/F87V/E143G/T152A/L188Q/E267V/Q403R/V413A
G2	R47L/F81I/F87V/E143G/L188Q/I219N/E267V
H1	I39V/R47L/F81I/F87V/E143G/L188Q/N213D/I259T/E267V
159	R47L/F81I/F87V/E143G/L188Q/L262F/E267V
172	R47L/F81I/F87V/E143G/L188Q/E267V/K309N
179	R47L/F81I/F87V/E143G/L188Q/N213S/E267V
198	R47L/F81I/F87V/E143G/F158L/L188Q/E267V
221	F11Y/R47L/F81I/F87V/E143G/L188Q/E267V/H408R
225	D23G/R47L/F81I/F87V/E143G/L188Q/E267V/E409D
250	R47L/F81I/F87V/E143G/L188Q/M212V/E267V/K309N
259	R47L/F81I/F87V/E143G/T149S/L188Q/E267V/S270G
301	R47L/F81I/F87V/S108C/E143G/T149S/L188Q/E267V
306	R47L/F81I/F87V/M112T/E143G/L188Q/E267V/M417T
326	R47L/F81I/F87V/K113E/E143G/T152S/L188Q/F261L/E267V

371	D23G/R47L/F81I/F87V/F107L/D136G/E143G/L188Q/E267V
375	R47L/F81I/F87V/S106C/Q109R/E143G/L188Q/E267V/D338E
380	R47L/F81I/F87V/L103F/D136G/E143G/N159S/L188Q/E267V
381	R47L/F81I/F87V/W96R/S106R/E143G/L188Q/E267V/I401V
387	F11L/R47L/F81I/F87V/Q110P/E143G/L188Q/R190Q/E267V
389	D23G/R47L/F81I/D84N/F87V/E143G/G154S/M185V/L188Q/E267V
413	R47L/F81I/F87V/Q128R/E143G/L188Q/E267V/L287S/K309R/S383C
416	R47L/S72C/F81I/F87V/S108G/E143G/F158L/L188Q/M212V/E267V/E344D

[a] Engineered CYP102A1 #1-16 were obtained by site-directed mutagenesis of the active site residues [1]. Engineered CYP102A1 #19-23 were obtained from random mutagenesis [2]. Chimera M16V2 was designed by domain exchange of the reductase domain of highly active mutants (#16) with that of the natural variants. Engineered CYP102A1 B10-#416 were obtained by random mutagenesis of heme domain of the chimera M16V2 [3,4].

References for supporting materials

1. Kim, D.H.; Kim, K.H.; Kim, D.H.; Liu, K.H.; Jung, H.C.; Pan, J.G.; Yun, C.H. Generation of human metabolites of 7-ethoxycoumarin by bacterial cytochrome P450 BM3. Drug Metab. Dispos. 2008, 36, 2166-2170.
2. Park, S. H.; Kim, D. H.; Kim, D.; Kim, D. H.; Jung, H. C.; Pan, J. G.; Ahn, T.; Kim, D.; Yun, C. H. Engineering bacterial cytochrome P450 (P450) BM3 into a prototype with human P450 enzyme activity using indigo formation. Drug Metab. Dispos. 2010, 38, 732-739.
3. Kang, J.Y.; Ryu, S.H.; Park, S.H.; Cha, G.S.; Kim, D.H.; Kim, K.H.; Hong, A.W.; Ahn, T.; Pan, J.G.; Joung, Y.H.; Kang, H.S.; Yun, C.H. Chimeric cytochromes P450 engineered by domain swapping and random mutagenesis for producing human metabolites of drugs. Biotechnol. Bioeng. 2014, 111, 1313-1322.
4. Jang, H.H.; Ryu, S.H.; Le, T.K.; Doan, T.T.; Nguyen, T.H.; Park, K. D.; Yim, D.E.; Kim, D.H.; Kang, C.K.; Ahn, T.; Kang, H.S.; Yun, C.H. Regioselective C-H hydroxylation of omeprazole sulfide by Bacillus megaterium CYP102A1 to produce a human metabolite. Biotechnol. Lett. 2017, 39, 105-112.